Strained Molecular Wires

DOI: 10.1002/ange.200801188

Enhanced π Conjugation around a Porphyrin[6] Nanoring**

*Markus Hoffmann, Joakim Kärnbratt, Ming-Hua Chang, Laura M. Herz, Bo Albinsson, and Harry L. Anderson**

Dedicated to Professor Jeremy Sanders on the occasion of his 60th birthday

Belt-shaped chromophores provide fascinating insights into electronic π delocalization over curved surfaces with radially oriented p orbitals.[1] Examples include the cyclic *para*-phenylacetylenes[2] and the [4$_6$]paracyclophanedodecayne of Tsuji and coworkers,[3] as well as fullerenes and carbon nanotubes. A variety of belt-shaped porphyrin arrays have been synthesized;[4] however, the vast majority of them lacks a complete π-conjugation pathway around the whole macrocycle. Recently we reported the synthesis of a belt-shaped D_{8h} symmetric porphyrin[8] nanoring on an octadentate template.[5] Herein we present an efficient synthesis of an even more strained π conjugated D_{6h} porphyrin[6] nanoring **1**, by template-directed trimerization of a porphyrin dimer **2** on a hexapyridyl template **3** (Scheme 1). This route is more direct than the synthesis of the cyclic octamer since both starting materials, **2** and **3**, are readily accessible. The cyclic hexamer complex **1·3** is phenomenally stable ($K_f = 7 \times 10^{38}\,\text{M}^{-1}$; $EM = 340\,\text{M}$) but the free macrocycle can be liberated from the **1·3** complex with amines such as quinuclidine. The UV/Vis/NIR absorption and emission show that there is efficient π conjugation around the porphyrin[6] nanoring **1**, and that its S_0–S_1 gap is even smaller than that of the corresponding linear porphyrin hexamer **4**; this conclusion is supported by time-dependent density functional (TD-DFT) calculations.

The key to the synthesis of the hexamer nanoring is the design of a complementary template (Scheme 2). The hexadentate template **3** has a calculated nitrogen–nitrogen distance of 20.1 Å, which is a good fit for the cavity of cyclic hexamer **1** with a zinc–zinc ring diameter of 24.2 Å (assuming a Zn–N bond length of 2.2 Å). The template was synthesized by a six-fold Suzuki coupling of 4-pyridineboronic acid with hexakis(4-bromophenyl)benzene[6] in 50% yield (Supporting Information). Two versions of cyclic hexamer **1** were synthesized—**1a·3** with *tert*-butyl side chains in 44% and **1b·3** with octyloxy side chains in 33% yield—by oxidative

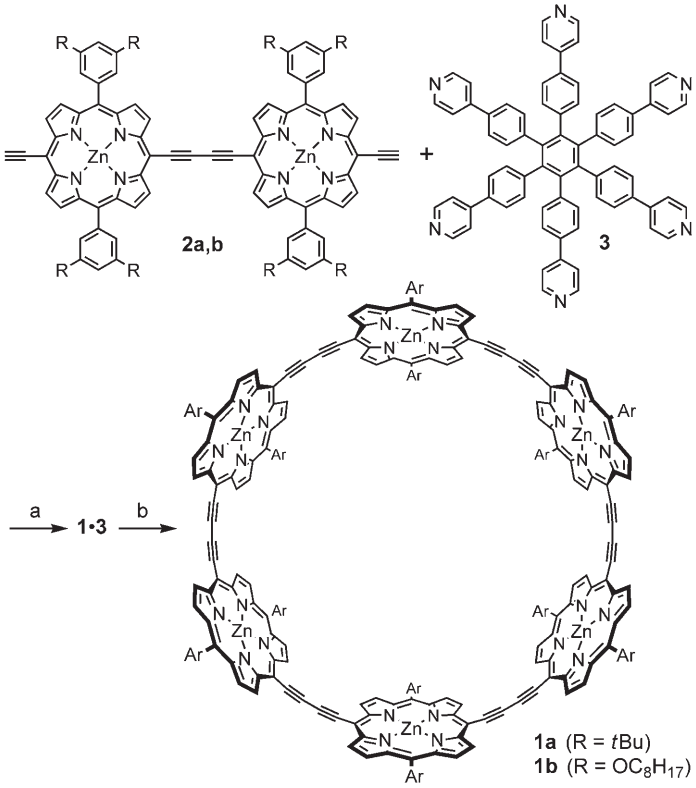

Scheme 1. Synthesis of porphyrin[6] nanorings **1a** and **1b**. Reagents: a) $[PdCl_2(PPh_3)_2]$, CuI, I_2, iPr_2NH, air, 60°C; (b) DABCO.

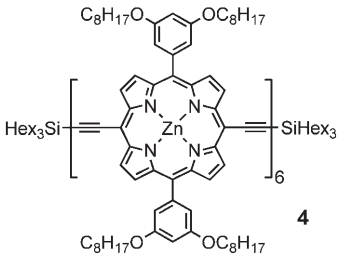

[*] M. Hoffmann, Prof. H. L. Anderson
Department of Chemistry, Oxford University
Chemistry Research Laboratory
12 Mansfield Road, Oxford OX1 3TA (UK)
Fax: (+44) 1865-28-5002
E-mail: harry.anderson@chem.ox.ac.uk
Homepage: http://users.ox.ac.uk/~hlagroup
M.-H. Chang, Dr. L. M. Herz
Department of Physics, Oxford University
J. Kärnbratt, Prof. B. Albinsson
Department of Chemical and Biological Engineering
Physical and Organic Chemistry, Chalmers University of Technology
Kemivägen 10, 41296 Göteborg (Sweden)

[**] This work was supported by EPSRC. We thank Johannes K. Sprafke for preliminary experiments on the synthesis of the template, and the EPSRC Mass Spectrometry Service (Swansea) for mass spectra.

Supporting information for this article is available on the WWW under http://dx.doi.org/10.1002/anie.200801188.

© 2008 Wiley-VCH Verlag GmbH & Co. KGaA, Weinheim

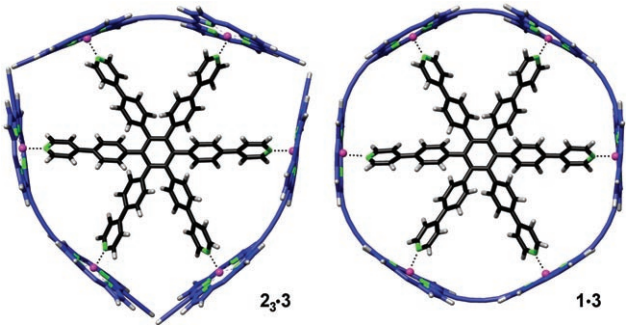

Scheme 2. Optimized geometries of $\mathbf{2}_3\cdot\mathbf{3}$ and **1·3**, calculated using the MM+ force field (*meso*-aryl substituents omitted for clarity).

coupling of porphyrin dimer **2a/b** under palladium/copper catalysis, using iodine and air as oxidants.[7] Size-exclusion chromatography in the presence of 1,4-diazabicyclo-[2.2.2]octane (DABCO) gave the template-free nanorings **1a** and **1b**.

^{1}H NMR spectroscopic analysis proves the high symmetry of **1·3** and **1** (Figure 1). Each compound gives just two sharp doublets for the β protons on the porphyrin units. The aryl and *t*Bu resonances in **1a·3** are split as the faces of the

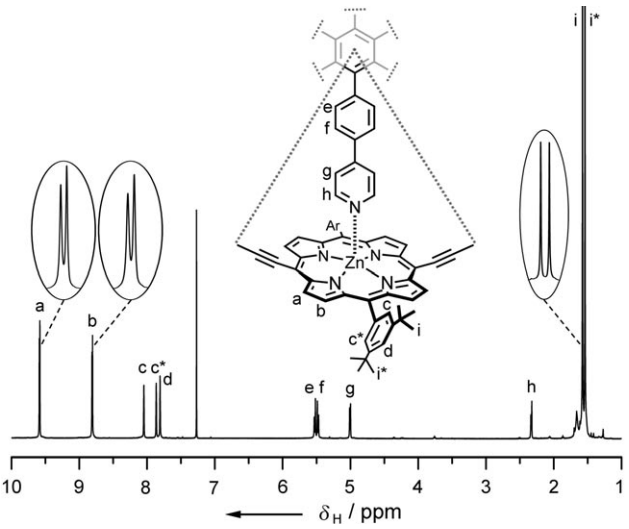

Figure 1. ^{1}H NMR spectrum of **1a·3** ($CDCl_3$, 298 K, 500 MHz).

porphyrin rings are nonequivalent with one side of each aryl substituent pointing towards the center of the ring. After removal of the template the faces of the porphyrin rings become equivalent, probably because the porphyrin units rotate rapidly on the NMR time-scale.

Previously, we reported that the template is displaced from our porphyrin[8] nanoring with pyridine.[5] However, pyridine does not displace the template from **1a·3** and **1b·3**, even when the complexes are dissolved in neat pyridine ([pyridine] = 12.4 M). More strongly coordinating amines, such as quinuclidine do displace the template from these complexes, when used in large excess ([quinuclidine] > 0.4 M; 250000 equiv).

Very large equilibrium constants for the formation of complexes—as in the case of **1·3**—can be measured by analyzing the thermodynamics of template displacement with a competing monodentate ligand.[5] Thus UV/Vis titrations were used to quantify the displacement of the template **3** from **1b·3**, and from the complex of the linear hexamer, **4·3**. All these titrations show simple isosbestic behavior, and the binding isotherms fit well to the calculated curves for two-state equilibria with K_b values of $4.5\times10^{-3}\,M^{-5}$ and $2.4\times10^{4}\,M^{-5}$ for **1b·3** and **4·3**, respectively, which correspond to K_f values of $(6.6\pm4.2)\times10^{38}\,M^{-1}$ and $(1.4\pm0.9)\times10^{21}\,M^{-1}$, respectively. Comparison of these two binding constants implies that the Gibbs energy required to bend the linear hexamer **4** into a cyclic conformation is 101 kJ mol^{-1}. The complementarity of template **3** to the porphyrin hexamers can be quantified by the effective molarity (EM) according to Equation (1), where K_0 is the binding constant of one arm of

$$EM = \sqrt[5]{K_f\,K_0^{-6}} \qquad (1)$$

the template for one site of the hexamer. K_0 can be approximated to the binding constant for 4-phenylpyridine and a 5,10-diethynylporphyrin zinc monomer ($K_0 = 2.3\times10^{4}\,M^{-1}$), which gives EM values of (340 ± 60) and (0.10 ± 0.02) M for **1b·3** and **4·3**, respectively. Each of these effective molarities is an average of five values, for coordination of the second, third, fourth, fifth, and sixth sites of the template to the porphyrin hexamer. The effective molarity for forming **1b·3** is an extremely high value for a noncovalent self-assembly process,[8] and it is consistent with the fact that pyridine is not able to displace the template.

To test how curvature changes the π conjugation in these wires, we compared the absorption and fluorescence spectra of the hexamer nanoring **1**, and its template complex **1·3**, with those of the linear hexamer **4** and its template complex **4·3** (Figure 2). The template-bound nanoring **1a·3** exhibits a sharp structured absorption band with maxima at 772, 809, and 850 nm, and a shoulder at 905 nm. The template-free cyclic hexamer **1a** has a similar multiplet pattern, although its spectrum is less well resolved, indicating greater conformational flexibility. The absorption spectrum of the linear hexamer **4** is much broader with a maximum at 804 nm, but when coordinated to the template to form **4·3** it splits into four peaks at 732, 781, 821, and 887 nm. The fluorescence spectra of **1a**, **1a·3**, and **4·3** (λ_{max} = 896, 914, and 894 nm, respectively) are significantly red-shifted compared to that of the linear hexamer **4** (λ_{max} = 827 nm), showing that the nanoring has a smaller S_0–S_1 gap and confirming that π conjugation is effective around these curved porphyrin wires.

Changing the geometry of the hexamer from linear to cyclic imposes symmetry-related constraints on the electronic transitions. This can be understood qualitatively in terms of a simple exciton model, assigning one transition dipole moment to each porphyrin (Scheme 3). The lowest-energy transition, corresponding to a head-to-tail arrangement of transition moments, is strong for the linear hexamer **4**, but forbidden for the nanoring **1** because the transition moments cancel. This model is of course very crude, but TD-DFT calculations give a

 © 2008 Wiley-VCH Verlag GmbH & Co. KGaA, Weinheim

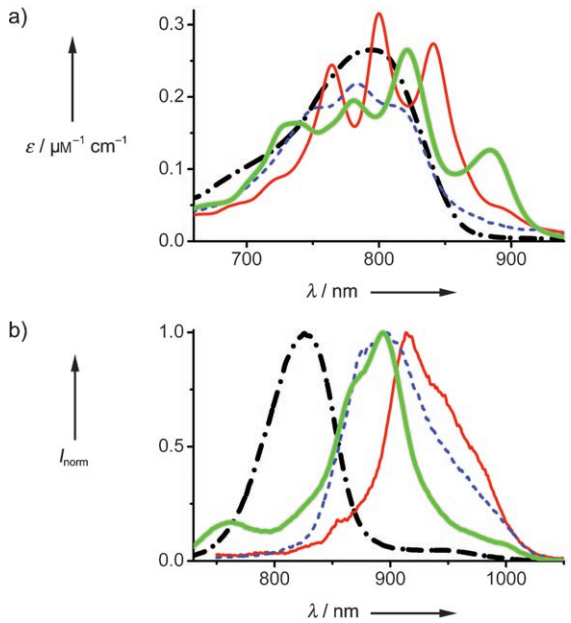

Figure 2. Vis/NIR absorption spectra (a) and emission spectra (b) of **1a·3** (red, plain) excited at 850 nm, **1a** (blue, dashed) excited at 870 nm, **4** (black, dotted-dashed) excited at 499 nm and **4·3** (green, bold) excited at 499 nm in toluene. 1% pyridine was added to **1a** and **4** to prevent aggregation. The weak emission spectra of **1a·3** and **1a** are slightly distorted from scattering of the excitation light. The small peak at 760 nm in the emission spectrum for **4·3** is due to a trace of a more fluorescent impurity. ε: extinction coefficient; I_{norm}: normalized photoluminescence.

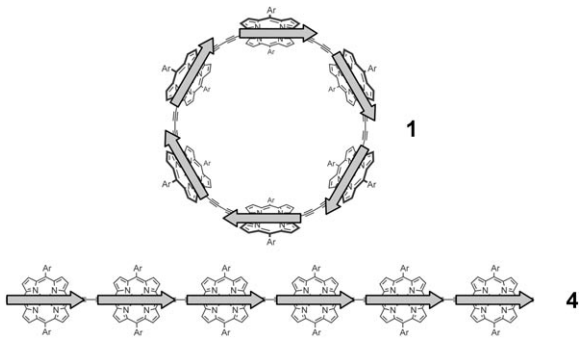

Scheme 3. Schematic representation of the transition dipole moment arrangement in the lowest $S_0 \rightarrow S_1$ transition of the cyclic hexamer **1** and linear hexamer **4**. The cancellation of the transition moments in **1** makes the lowest electronic transition symmetry-forbidden.

similar picture (Supporting Information), predicting a forbidden $S_0 \rightarrow S_1$ transition followed by a strongly allowed $S_0 \rightarrow S_2$ transition. Several experimental observations corroborate this model. First, the total lack of mirror symmetry between the absorption and emission spectra of **1a·3** points to a complex absorption band composed of several electronic transitions rather than a vibronic progression. Second, the fluorescence quantum yield Φ_f drops from 0.08 to 0.002 when comparing **4** and **1a** and the radiative rate constant k_f decreases by nearly two orders of magnitude (Table 1), indicating a dramatic reduction in the S_0–S_1 oscillator strength in the nanoring. Conformational flexibility evidently relaxes this symmetry-related selection rule: the nanoring–template complex **1a·3** with the most rigid symmetrical structure has the lowest quantum yield and shows the slowest radiative decay; both parameters increase in the more flexible free nanoring **1**, and in the less symmetrical complex **4·3**.

Further insights into the electronic structure are provided by comparing the observed radiative rate constants with those estimated from the absorption spectra through the Strickler–Berg relation,[9] where ν is the transition frequency and ε is the

$$k_f = 2.88 \times 10^{-9} \nu^2 \int \varepsilon(\nu) d\nu \qquad (2)$$

molar absorptivity. The radiative rate constants, k_f, were estimated from the absorption spectra first assuming that the whole Q-band at 650–950 nm corresponds to the S_0–S_1 transition (Table 1). The results from the Strickler–Berg relation are in agreement with the observed radiative rate constant for the linear hexamer, but are greatly overestimated for the other compounds. A much better agreement for the cyclic structures is achieved if only the weak most red-shifted peak in the absorption spectrum is considered.[10] This confirms that the S_0–S_1 transitions for the cyclic structures are weakly allowed and lie at around 900 nm, as suggested by the exciton model and the TD-DFT calculations.

In summary, we have synthesized a strained π conjugated porphyrin nanoring by template-directed trimerization of a porphyrin dimer. The effective molarity (ca. 300 M) for forming the complex **1b·3** is exceptionally high. Absorption and emission spectra show that π conjugation is more effective in the nanoring than in its linear analogue. Thus the $S_1 \rightarrow S_0$ fluorescence band shifts from 827 nm in the linear hexamer to ca. 900 nm in the cyclic hexamers. DFT calculations corroborate the enhanced π conjugation in the nanoring, and show that the S_0–S_1 transition is forbidden, accounting for the low radiative rate constant of the nanoring. The enhanced conjugation in the nanoring probably results from its rigid geometry and from the lack of end-effects, perhaps with a contribution from out-of-plane distortion of

Table 1: Quantum yields Φ_f, fluorescence lifetimes τ_f, and radiative rate constants k_f.

	Φ_f	τ_f [ps]	k_f [s^{-1}][a]	k_f [s^{-1}][b]	k_f [s^{-1}][c]
4	0.08	650	1.3×10^8	2.7×10^8	
4·3	0.006	500	1.2×10^7	1.9×10^8	2.1×10^7
1a·3	0.001	340	2.9×10^6	2.2×10^8	7.7×10^6
1a	0.002	460	4.3×10^6	1.9×10^8	8.1×10^6

[a] Calculated from Φ_f/τ_f. [b] Calculated from Equation (2) with an integrated absorptivity between 650 and 950 nm. [c] Calculated from Equation (2) where only the most red-shifted peak in the absorption is considered.[10]

© 2008 Wiley-VCH Verlag GmbH & Co. KGaA, Weinheim

the π system. The structural similarity between the arrangement of porphyrin chromophores in these nanorings and that of chlorophyll units in the natural LH2 light-harvesting system,[11] and the strong electronic coupling between the porphyrin units, makes it interesting to explore the exciton delocalization in these nanorings using ultra-fast time-resolved techniques. These experiments are now in progress.

Received: March 12, 2008
Revised: April 26, 2008
Published online: May 28, 2008

Keywords: conjugation · molecular electronics · porphyrinoids · self-assembly · template synthesis

[1] For reviews see: a) T. Kawase, H. Kurata, *Chem. Rev.* **2006**, *106*, 5250 – 5273; b) K. Tahara, Y. Tobe, *Chem. Rev.* **2006**, *106*, 5274 – 5290; c) L. T. Scott, *Angew. Chem.* **2003**, *115*, 4265 – 4267; *Angew. Chem. Int. Ed.* **2003**, *42*, 4133 – 4135.

[2] T. Kawase, H. R. Darabi, M. Oda, *Angew. Chem.* **1996**, *108*, 2803 – 2805; *Angew. Chem. Int. Ed. Engl.* **1996**, *35*, 2664 – 2666.

[3] M. Ohkita, K. R. Ando, T. Tsuji, *Chem. Commun.* **2001**, 2570 – 2571.

[4] a) S. Anderson, H. L. Anderson, J. K. M. Sanders, *Acc. Chem. Res.* **1993**, *26*, 469 – 475; b) S. Rucareanu, A. Schuwey, A. Gossauer, *J. Am. Chem. Soc.* **2006**, *128*, 3396 – 3413; c) J. Li, A. Ambroise, S. I. Yang, J. R. Diers, J. Seth, C. R. Wack, D. F. Bocian, D. Holten, J. S. Lindsey, *J. Am. Chem. Soc.* **1999**, *121*, 8927 – 8940; d) Y. Kuramochi, A. Satake, Y. Kobuke, *J. Am. Chem. Soc.* **2004**, *126*, 8668 – 8669; e) T. Hori, N. Aratani, A. Takagi, T. Matsumoto, T. Kawai, M.-C. Yoon, Z. S. Yoon, S. Cho, D. Kim, A. Osuka, *Chem. Eur. J.* **2006**, *12*, 1319 – 1327.

[5] M. Hoffmann, C. J. Wilson, B. Odell, H. L. Anderson, *Angew. Chem.* **2007**, *119*, 3183 – 3186; *Angew. Chem. Int. Ed.* **2007**, *46*, 3122 – 3125.

[6] R. Rathore, C. L. Burns, M. I. Deselnicu, *Org. Lett.* **2001**, *3*, 2887 – 2890.

[7] a) J. A. Marsden, J. J. Miller, M. M. Haley, *Angew. Chem.* **2004**, *116*, 1726 – 1729; *Angew. Chem. Int. Ed.* **2004**, *43*, 1694 – 1697; b) A. S. Batsanov, J. C. Collings, I. J. S. Fairlamb, J. P. Holland, J. A. K. Howard, Z. Lin, T. B. Marder, A. C. Parsons, R. M. Ward, J. Zhu, *J. Org. Chem.* **2005**, *70*, 703 – 706.

[8] a) P. Ballester, A. I. Oliva, A. Costa, P. M. Deya, A. Frontera, R. M. Gomila, C. A. Hunter, *J. Am. Chem. Soc.* **2006**, *128*, 5560 – 5569; b) V. M. Krishnamurthy, V. Semetey, P. J. Bracher, N. Shen, G. M. Whitesides, *J. Am. Chem. Soc.* **2007**, *129*, 1312 – 1320; c) G. Ercolani, *Struct. Bonding (Berlin)* **2006**, *121*, 167 – 215.

[9] S. J. Strickler, R. A. Berg, *J. Chem. Phys.* **1962**, *37*, 814 – 822.

[10] The integrated absorptivity of the most red-shifted component of the Q-band was calculated from an estimate of the width of the band. Since this transition overlaps heavily with the rest of the Q-band, this estimate may be inaccurate but it is good enough for the qualitative analysis presented here.

[11] a) G. McDermott, S. M. Prince, A. A. Freer, A. M. Hawthornthwaite-Lawless, M. Z. Papiz, R. J. Cogdell, N. W. Isaacs, *Nature* **1995**, *374*, 517 – 521; b) Y. Nakamura, N. Aratani, A. Osuka, *Chem. Soc. Rev.* **2007**, *36*, 831 – 845.

 © 2008 Wiley-VCH Verlag GmbH & Co. KGaA, Weinheim